

# Event-by-Event Efficiency Fluctuations and Efficiency Correction for Cumulants of Superposed Multiplicity Distributions in Relativistic Heavy-ion Collision Experiments

Shu He<sup>1</sup> and Xiaofeng Luo<sup>1,\*</sup>

<sup>1</sup>*Key Laboratory of Quark & Lepton Physics (MOE) and Institute of Particle Physics, Central China Normal University, Wuhan 430079, China*

We performed systematic studies for the effects of event-by-event efficiency fluctuations on efficiency correction for cumulant analysis in relativistic heavy-ion collision experiments. Experimentally, particle efficiencies of events measured with different experimental conditions should be different. For fluctuation measurements, the final event-by-event multiplicity distributions should be the superposed distributions of various type of events measured under different conditions. We demonstrate the efficiency fluctuation effects in a numerical simulation, in which we construct an event ensemble consists of events with two different efficiencies. By using the mean particle efficiencies, we find the efficiency corrected cumulants show large deviations from the original inputs when the discrepancy of the two efficiencies are large. We further studied the effects of efficiency fluctuations for the cumulants of net-proton distributions by implementing the UrQMD events of Au+Au collisions at  $\sqrt{s_{NN}} = 7.7$  GeV in a realistic STAR detector acceptance. We consider the unequal efficiency in two sides of the Time Projection Chamber (TPC), multiplicity dependent efficiency and the event-by-event variations of the collision vertex position along the longitudinal direction ( $V_z$ ). When the efficiencies fluctuate dramatically within the studied event sample, the effects of efficiency fluctuations have significant impacts on the efficiency corrections of cumulants with the mean efficiencies. We find that this effect can be effectively suppressed by binning the entire event ensemble into various sub-event samples, in which the efficiency variations are relative small. The final efficiency corrected cumulants can be calculated from the weighted average of the corrected factorial moments of the sub-event samples with the mean efficiencies.

## I. INTRODUCTION

The major physics goals of heavy-ion collision experiment are to explore the phase structure of strongly interacting nuclear matter and study the properties of quark-gluon plasma (QGP), which consists of deconfined quarks and gluons. The quantum chromodynamics (QCD) is the theory for strong interaction. The QCD phase structure can be displayed in the phase diagram, which describes the state of matter at given external parameters. Two most important external parameters to QCD phase transition are the temperature  $T$  and baryon number density or baryon chemical potential  $\mu_B$ . In the conjecturing QCD phase diagram, the Lattice QCD calculation shows that the phase transition from hadronic phase to QGP phase at zero  $\mu_B$  is crossover [1], meanwhile several QCD based models suggest that at larger  $\mu_B$ , the transition is of first order [2, 3]. If the those calculations are true, there should exist an endpoint of first order transition line, which is so called the QCD critical point. Due to the sign problem of Lattice QCD at  $\mu_B > 0$ , the first-principle calculation become very difficult for QCD critical point search [4] and there has large uncertainties of the location of the critical point in theoretical study [5–15].

One of the most important experimental method of searching for the critical point is the measurements of the event-by-event fluctuations of conserved quantity, such as net-baryon ( $B$ ) [16–18], net-charge number ( $Q$ ) [19, 20] and net-strangeness ( $S$ ) number [21–39] (And their proxy observables net-kaon [40] and net-proton number fluctua-

tions). The fluctuation observables are sensitive to the correlation length  $\xi$ , which will diverge near the QCD critical point. The Solenoidal Tracker at RHIC (STAR) experiment has measured the fluctuation of net-proton multiplicity (which is a proxy to net-baryon) in Au + Au collisions at  $\sqrt{s_{NN}} = 7.7, 11.5, 14.5, 19.6, 27, 39, 62.4$  and 200 GeV, which is taken from the first phase of RHIC beam energy scan program. The measured fourth order cumulants ratio ( $\kappa\sigma^2 = C_4/C_2$ ) of 5% most central events shows a non-monotonic energy (or  $\mu_B$ ) dependence [41–43].

To understand the physics behind this measurement, we need to perform careful studies on the background contributions, such as detector efficiency and acceptance effects, volume fluctuations and other non-critical physics [44–52]. Due to finite detector efficiency, efficiency correction has been applied and plays a very important role in the cumulant analysis. Generally, the efficiencies are obtained by Monte Carlo (MC) embedding technique [53]. It gives the efficiency which is the ratio of matched MC tracks number and the number of input tracks. It contains the effects of both reconstructed tracking efficiency and acceptance, which reflects the mean properties of the entire event ensemble. However, the problem is that the higher order cumulants are sensitive statistics, it receives impact from bulk properties of events. Particle efficiencies of events measured with different experimental conditions should be different. The final event-by-event multiplicity distributions should be the superposed distributions of various type of events measured under different conditions. However, the efficiency correction is done with a mean efficiency of the event sample. The average quantity on event ensemble will drop the detail of event-by-event discrepancy, which could be crucial to the cumulants analysis, for example, the

\* xfluo@mail.ccnu.edu.cn

efficiency and acceptance may fluctuate event from event when the position of collision vertexes are different. So, it is important to quantify and/or correct for the effects of event-by-event fluctuation efficiency on efficiency corrections of cumulants.

This paper is organized as follow. In the Section II we will introduce the cumulants observables and the efficiency correction to cumulants. In the Section III we will show the effects of using mean efficiency with a numerical simulation. In the Section IV, the effects of using mean efficiency are tested by events generated from UrQMD model with a fast detector simulation. Finally, we will give a summary.

## II. CUMULANTS AND EFFICIENCY CORRECTION

The cumulants of conserved charge are sensitive probes to QCD phase transition and the QCD critical point, the fourth order cumulant is proportional to the seventh order of correlation length  $C_4 \propto \xi^7$ . The cumulants  $C_1 \sim C_4$  can be defined by moments  $\langle N \rangle, \langle N^2 \rangle, \dots, \langle N^4 \rangle$  as:

$$\begin{aligned} C_1 &= \langle N \rangle \\ C_2 &= \langle N^2 \rangle - \langle N \rangle^2 \\ C_3 &= 2 \langle N \rangle^2 - 3 \langle N \rangle \langle N^2 \rangle + \langle N^3 \rangle \\ C_4 &= -6 \langle N \rangle^4 + 12 \langle N \rangle^2 \langle N^2 \rangle - 3 \langle N^2 \rangle^2 \\ &\quad - 4 \langle N \rangle \langle N^3 \rangle + \langle N^4 \rangle \end{aligned} \quad (1)$$

The variance  $\sigma^2$ , skewness  $S$  and kurtosis  $\kappa$  can be defined as

$$\sigma^2 = C_2, \quad S = \frac{C_3}{(C_2)^{3/2}}, \quad \kappa = \frac{C_4}{C_2^2}$$

The ratios of cumulants can be directly compared to the thermodynamic susceptibilities, which can be computed in Lattice QCD [22].

$$S\sigma = \frac{C_3}{C_2} = \frac{\chi_4}{\chi_2}, \quad \kappa\sigma^2 = \frac{C_4}{C_2} = \frac{\chi_3}{\chi_2}$$

The cumulants measured with detector efficiencies can be recovered by efficiencies correction. For example, the mean value can be corrected by

$$\langle N \rangle = \frac{\langle N \rangle_{\text{measure}}}{\epsilon}, \quad \langle N - \bar{N} \rangle = \frac{\langle N \rangle}{\epsilon_{\text{proton}}} - \frac{\langle \bar{N} \rangle}{\epsilon_{\text{anti-proton}}}$$

Typically, the efficiencies for proton and anti-proton are different. Thus, we should divide the mean value by corresponding efficiency respectively.

The efficiency corrections for higher order cumulants are not quite straightforward, one can assume that the response function of detecting particles follows the binomial distribution with efficiency parameter  $\epsilon$ . Then we can express the moments in terms of factorial moments [54, 55]. The  $r$ -th order factorial moments of a stochastic variable  $N$  can be defined from expectation of its falling factorial

$$F_r = \langle N(N-1)\cdots(N-r+1) \rangle$$

And the factorial moments can be easily corrected for the binomial efficiency. Suppose the measured factorial moment is  $f_r$  with efficiency  $\epsilon$ , we have (Section VIA)

$$F_r = \frac{f_r}{\epsilon^r} \quad (2)$$

With the efficiency corrected factorial moments  $F_1$  to  $F_r$ , we can write down the moments  $\langle N^r \rangle$

$$\langle N^r \rangle = \sum_{i=0}^r s_2(r, i) F_i \quad (3)$$

Where the  $s_2$  is the Stirling numbers of the second kind. With moments  $\langle N^r \rangle$  we can further write down the cumulants with equation (1). In the case where net-proton cumulants is required, we should introduce 2-dimensional factorial and the efficiency correction equation become

$$F_{rs} = \frac{f_{rs}}{\epsilon_p^r \epsilon_{\bar{p}}^s}$$

Where the  $\epsilon_p^r$  is the  $r$ -th order of proton efficiency and the  $\epsilon_{\bar{p}}^s$  is the  $s$ -th order of anti-proton efficiency. And  $f_{rs}$  is defined as

$$f_{rs} = \langle n_p(n_p-1)\cdots(n_p-r+1) \cdot n_{\bar{p}}(n_{\bar{p}}-1)\cdots(n_{\bar{p}}-s+1) \rangle \quad (4)$$

Where  $n_p$  and  $n_{\bar{p}}$  are the measured proton and anti-proton number. The conversion from  $F_{rs}$  to  $\langle N_p^r N_{\bar{p}}^s \rangle$  is

$$\langle N_p^r N_{\bar{p}}^s \rangle = \sum_{i_1=0}^r \sum_{i_2=0}^s s_2(r, i_1) s_2(s, i_2) F_{r_1 s_2}$$

The moments of net-proton can be expressed as

$$\begin{aligned} \langle N_{p-\bar{p}}^k \rangle &= \langle (N_p - N_{\bar{p}})^k \rangle \\ &= \sum_{i=0}^k (-1)^i \binom{k}{i} \langle N_p^{k-i} N_{\bar{p}}^i \rangle \end{aligned} \quad (5)$$

It is straightforward to write the net-proton cumulants with equation (1).

### A. Factorial moments and cumulants of superposed distribution

In this section, we discuss the factorial moments of superposed distribution. For example, if we have a distributions obtained by the mixture of the Poisson distribution, Gaussian distribution, or some distributions of other types. The question is what's the relations between the factorial moments of their superposed distribution and the sub-distributions. The probability density function of superposed distribution can be expressed as:

$$\tilde{P}(n) = \sum a_i P_i(n) \quad (6)$$

It describes the probability of detecting  $n$  particles in an event, and the event may be from one of the various types. Therefore,  $\tilde{P}(n)$  is the summation of probability of detecting  $n$  particles from the  $i$ -th type  $P_i(n)$ . The  $a_i$  is the weight of  $P_i(n)$

With  $\tilde{P}(n)$ , we can write down the generating function  $\tilde{G}_F(s)$  for factorial moments  $F_r$

$$\begin{aligned}\tilde{G}_F(s) &= \sum_{n=0}^{\infty} \tilde{P}(n) s^n \\ &= \sum_{n=0}^{\infty} \sum_{i=0}^k a_i P_i(n) s^n\end{aligned}\quad (7)$$

We can further write

$$\tilde{G}_F(s) = \sum_{i=0}^k a_i \sum_{n=0}^{\infty} P_i(n) s^n = \sum_{i=0}^k a_i G_F^{(i)}(s) \quad (8)$$

We then have the relation between superposed factorial moments  $\tilde{F}_r$  and  $F_r^{(i)}$

$$\begin{aligned}\tilde{F}_r &= \left. \frac{\partial^r}{\partial s^r} \tilde{G}_F(s) \right|_{s=1} \\ &= \sum_{i=0}^k a_i \left. \frac{\partial^r}{\partial s^r} G_F^{(i)}(s) \right|_{s=1} \\ &= \sum_{i=0}^k a_i F_r^{(i)}\end{aligned}\quad (9)$$

We find  $\tilde{F}_r$  is the weighted average of  $F_r^{(i)}$ .

However, we will show we can not use the average of cumulants from different types of distributions. First, we note that the superposed cumulants  $\tilde{C}_r$  is not the simple weighted average of  $C_r^{(i)}$ . Since generating function of cumulants  $K(\theta)$  can be written as [56]

$$K(\theta) = K_{fc}(e^\theta) \quad (10)$$

The  $K_{fc}(e^\theta)$  is the generating function of factorial cumulants, and we have

$$K_{fc}(e^\theta) = \ln G_F(e^\theta) \quad (11)$$

Therefore

$$K(\theta) = \ln G_F(e^\theta) \quad (12)$$

The generating function of superposed distribution is

$$\tilde{K}(\theta) = \ln \tilde{G}_F(e^\theta) = \ln \sum_{i=0}^k a_i G_F^{(i)}(e^\theta) \quad (13)$$

The cumulants  $\tilde{C}_r$  are given by

$$\begin{aligned}\tilde{C}_r &= \left. \frac{\partial^r}{\partial \theta^r} \tilde{K}(\theta) \right|_{\theta=0} \\ &= \left. \frac{\partial^r}{\partial \theta^r} \ln \sum_{i=0}^k a_i G_F^{(i)}(e^\theta) \right|_{\theta=0}\end{aligned}$$

$$\begin{aligned}&\neq \left. \frac{\partial^r}{\partial \theta^r} \sum_{i=0}^k a_i \ln G_F^{(i)}(e^\theta) \right|_{\theta=0} \\ &= \sum_{i=0}^k a_i \left. \frac{\partial^r}{\partial \theta^r} K^{(i)}(\theta) \right|_{\theta=0} = \sum_{i=0}^k a_i C_r^{(i)}\end{aligned}\quad (14)$$

Thus, if the individual distributions are different, the cumulant of the superposition of different distributions are not the average of the cumulants of the individual distributions.

Suppose  $G_F(e^\theta)$  is the factorial moments generating function after efficiency correction. Therefore, the superposed cumulants generating function is

$$\begin{aligned}\tilde{K}(\theta) &= \ln \tilde{G}_F(e^\theta) = \ln \sum_{i=0}^k a_i G_F^{(i)}(e^\theta) \\ &= \ln \sum_{i=0}^k a_i G_F(e^\theta) \\ &= \ln G_F(e^\theta) \\ &= \sum_{i=0}^k a_i \ln G_F(e^\theta) \\ &= \sum_{i=0}^k a_i K^{(i)}(\theta)\end{aligned}\quad (15)$$

We find that this relation is only true when all the  $G_F^{(i)}$  are equal. In other words, cumulants average can only valid for the superposed distributions of the same type.

The statistical error for superposed cumulants is given by the Delta theorem [55, 57]. In our discussion, the detecting efficiency  $\epsilon$  is taken as a constant. Therefore we have

$$\begin{aligned}V(\tilde{C}_r) &= \sum_{p,q} \frac{\partial \tilde{C}_r}{\partial \tilde{f}_p} \frac{\partial \tilde{C}_r}{\partial \tilde{f}_q} \text{Cov}(\tilde{f}_p, \tilde{f}_q) \\ &= \sum_{p,q} \sum_i \frac{\partial \tilde{C}_r}{\partial f_p^{(i)}} \frac{\partial \tilde{C}_r}{\partial f_q^{(i)}} \text{Cov}(f_p^{(i)}, f_q^{(i)})\end{aligned}\quad (16)$$

## B. Efficiency correction for superposed distribution with different efficiencies

Experimental measured multiplicity distribution can be treated as a superposed of distributions with different efficiencies. For simplicity, we assume the response function of the detecting efficiency is binomial distribution. This is a special case of equation (6), where  $p_i(n)$  is given by equation (28) with different efficiency  $\epsilon_i$

$$p_i(n) = \sum_{N=n}^{\infty} P(N) B_N(n, \epsilon_i) \quad (17)$$

and the PDF for superposed distribution is

$$\tilde{p}(n) = \sum_{i=0}^k a_i p_i(n) = \sum_{i=0}^k \sum_{N=n}^{\infty} a_i P(N) B_N(n, \epsilon_i) \quad (18)$$

The generating function of measured factorial moments for each species of distribution is given by equation (30)

$$\begin{aligned}
G_f^{(i)}(s) &= \sum_{n=0}^{\infty} p_i(n) s^n = \sum_{n=0}^{\infty} \sum_{N=n}^{\infty} P(N) B_N(n, \epsilon_i) s^n \\
&= \sum_{N=0}^{\infty} P(N) [1 + \epsilon_i (s-1)]^N \\
&= \sum_{N=0}^{\infty} P(N) s_i'^N = G_F(s_i') \quad (19)
\end{aligned}$$

where the  $s_i' = 1 + \epsilon_i (s-1)$ . And their average is given by equation (8), we have

$$\begin{aligned}
\tilde{G}_f(s) &= \sum_i^k a_i G_f^{(i)}(s) \\
&= \sum_i^k a_i G_F(s_i') \quad (20)
\end{aligned}$$

Then, we have the relation between measured factorial moments  $\tilde{f}_r$  and the original factorial moments from each species of event

$$\begin{aligned}
\tilde{f}_r &= \left. \frac{\partial^r}{\partial s^r} \tilde{G}_f(s) \right|_{s=1} \\
&= \sum_i^k a_i \left( \frac{\partial s_i'}{\partial s} \right)^r \left. \frac{\partial^r}{\partial (s_i')^r} G_F(s_i') \right|_{s=1} \\
&= \sum_i^k a_i \epsilon_i^r \left. \frac{\partial^r}{\partial (s_i')^r} G_F(s_i') \right|_{s_i'=1} \\
&= \sum_i^k a_i \epsilon_i^r F_r \quad (21)
\end{aligned}$$

The mean efficiency  $\langle \epsilon \rangle$  should not be used for the superposed distribution. It can be demonstrated in equation (21) by multiple  $1/\langle \epsilon \rangle$  to the both side and compare it to the original superposed factorial moments

$$\begin{aligned}
\frac{\tilde{f}_r}{\langle \epsilon \rangle^r} - F_r &= \sum_i^k a_i \frac{\epsilon_i^r}{\langle \epsilon \rangle^r} F_r - F_r \\
&= F_r \left( \frac{\sum_i^k a_i \epsilon_i^r}{\langle \epsilon \rangle^r} - 1 \right) \\
&= F_r \left( \frac{\langle \epsilon^r \rangle}{\langle \epsilon \rangle^r} - 1 \right) \quad (22)
\end{aligned}$$

Since  $\epsilon_i$  are fluctuating, the last line is usually not equal to 0. Ideally, in order to obtain factorial moments of original distribution, we should do efficiency correction for each types of events, separately:

$$F_r = \sum_{i=0}^k a_i \frac{f_r^{(i)}}{\epsilon_i^r} \quad (23)$$

There are two methods to obtain the efficiency corrected cumulants for superposed distribution from distributions with different efficiencies:

1. Correct  $f_r^{(i)}$  to  $F_r^{(i)}$  and compute  $C_r^{(i)}$ . Then  $\tilde{C}_r = \sum_i a_i C_r^{(i)}$ .
2. Correct  $f_r^{(i)}$  to  $F_r^{(i)}$ , and  $\tilde{F}_r = \sum_i a_i F_r^{(i)}$ . Then compute  $\tilde{C}_r$  from  $\tilde{F}_r$

If we know the efficiencies of different event types in the superposed distribution, we should note that after efficiency correction  $F_r^{(1)} = F_r^{(2)} = \dots = F_r^{(k)}$ . Therefore we can demonstrate that the method 1 and 2 are equivalent. However, in the Section IV C, we will find the efficiencies of each type of events are unknown. What we use is the mean  $\epsilon$  in each sub-event sample. Thus, the generating functions  $G_F^{(i)}$  in different event sample bins after efficiency correction are still not the same.  $G_F^{(i)}$  is only an approximation to the true  $G_F$ . Thus, the superposition of different types of distributions should be done with factorial moments average (method 2). If the efficiency variation in each bin is not small, the weight average of cumulants will introduce additional uncertainties.

### III. EFFECTS OF USING MEAN EFFICIENCY IN EFFICIENCY CORRECTION FOR CUMULANTS OF MULTIPLICITY DISTRIBUTIONS

Usually, the efficiency  $\epsilon$  in equation (2) obtained from MC embedding. It reflects the net contribution of detector acceptance, tracking efficiency and the other effects. It is obtained by taking average on the entire event ensemble. For most situations, the true efficiency of each event should not fluctuate too far from this mean value. In these cases, the  $\langle \epsilon \rangle$  is a good approximation for using in efficiency correction. But what if the efficiencies of some events are dramatically deviating from  $\langle \epsilon \rangle$ . Certainly, we can exclude bad events by rejecting events with unusual multiplicity or select events within a multiplicity range. However, with a relative large efficiency shift, the change in  $\langle N \rangle$  can be slight because the binomial distribution is wide. Thus, the event selection become difficult.

The problem of using mean efficiency to correct cumulants is realistic. We can consider an extreme example in which an event ensemble mixes up two types of distinctive events. One type of event has efficiency  $\epsilon_1$ , the other type has efficiency  $\epsilon_2$ . And the mean efficiency eventually is the average of two types of event  $\bar{\epsilon}$ . To model this example, we have done a Monte Carlo simulation. For each event, the proton number  $N$  we input follows the Poisson distribution with parameter  $\lambda = 100$ . In events of type I, the detected proton number  $n$  follows the binomial distribution  $B(N, \epsilon_1)$ . In events of type II, the  $n$  follows  $B(N, \epsilon_2)$ . The event-by-event proton number distributions from the simulation shown in Fig. 1.

In Figure. 1, we give the same original input distribution with the number of events ( $M$ ) for each case (the solid grey lines). We divide the input original events into two sub-event samples, which passes different efficiencies. The two types of events represented by type I and II with the number of events  $M_1$  and  $M_2$ , respectively ( $M_1 + M_2 = M$ ). The

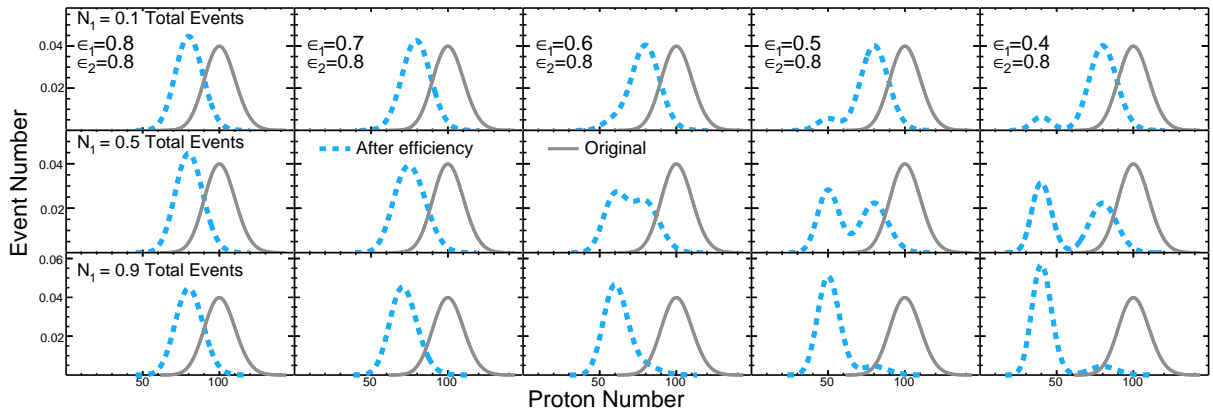


FIG. 1. Monte Carlo input (Original, gray line) and measured distribution with detector efficiencies (dashed blue line). The statistics of event is 1.0 billion ( $10^9$ ). In the first, second and third row, events with efficiency  $\epsilon_1$  (i.e. Events of type I) makes up 10%, 50% and 90% of total event number. In columns 1 to 5, the  $\epsilon_1$  varies from 0.8 to 0.4, while efficiency of type II is fixed at  $\epsilon_2 = 0.8$ .

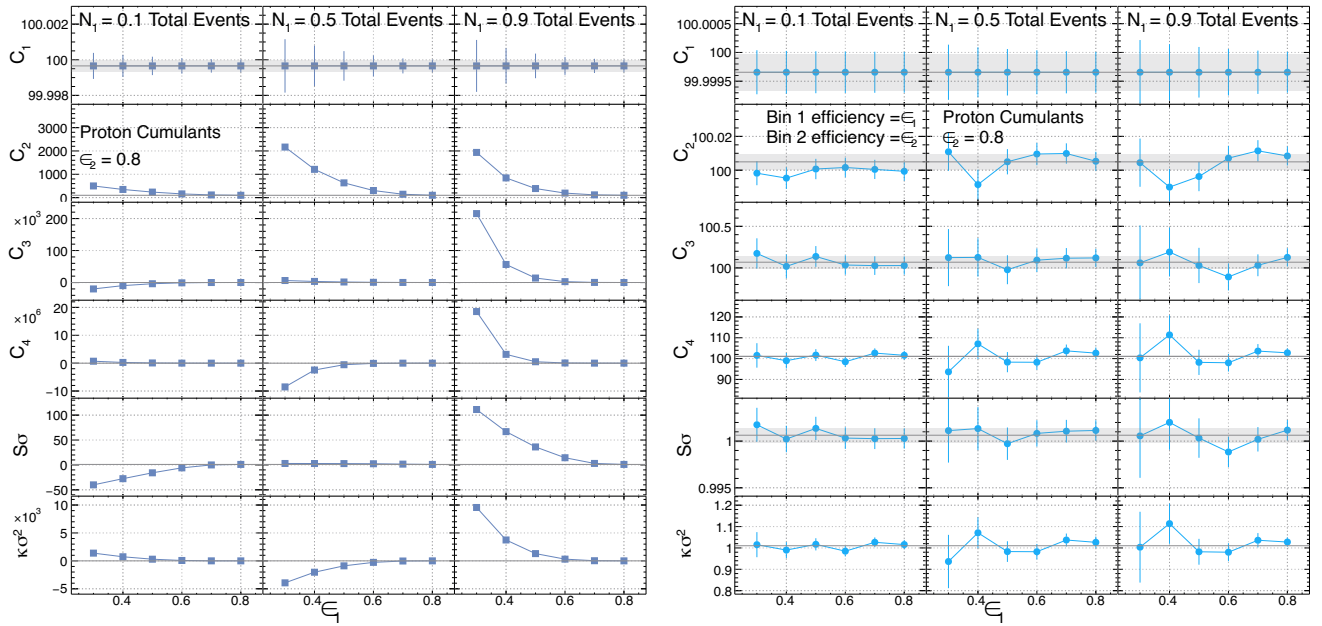


FIG. 2. Efficiency corrected cumulants and cumulants ratios. For each column, the events of type I makes up 10%, 50% and 90% of total event number ( $10^9$ ). The  $\epsilon_1$  in  $x$ -axis represents the efficiency event type I and the efficiency of type II is fixed at  $\epsilon_2 = 0.8$ . **Square markers** (left): Result corrected with mean efficiency. **Circle markers** (right): Result corrected independently by  $\epsilon_1$  and  $\epsilon_2$  (True efficiencies).

efficiency of type II is fixed at  $\epsilon_2 = 0.8$ . From column 1 to 5, we decrease the efficiency of type I events from 0.8 to 0.4. We find that the distinctive peaks of event-by-event distribution have gradually emerged. The event fraction of total events for type I sub-event sample are varied to be 0.1, 0.5, and 0.9. Then, we perform efficiency correction by using mean efficiency  $\langle \epsilon \rangle$  of each case. Since we can represent  $\epsilon_1$  by  $\epsilon_1 = \langle N \rangle_{\text{measure}} / \langle N \rangle_{\text{input}}$  and so is  $\epsilon_2$ , their average can be written as

$$\langle \epsilon \rangle = \frac{M_1 \langle n \rangle_1 + M_2 \langle n \rangle_2}{M \langle N \rangle}$$

Where the  $M_1$  is the number of events in type I and  $M_2$  is the

number of events in type II. The measured particle number is denoted as  $\langle n \rangle$ , and the input particle number is denoted as  $\langle N \rangle$ .

With the measured distributions (blue dashed lines in Fig. 1) and the mean efficiency  $\langle \epsilon \rangle$ , we can calculate the efficiency corrected factorial moments (equation (2)) and the cumulants, which are shown in Fig. 2 (left) as blue square marker. We tune the efficiency difference  $\Delta \epsilon$  of two types of events to see how the efficiency corrected results deviate from the original cumulants (marked as the solid gray lines). We found there is no problem to use mean efficiency in correction of  $C_1$ , since the results perfectly follow the solid lines (approximately around 100.0 which is the Poisson param-

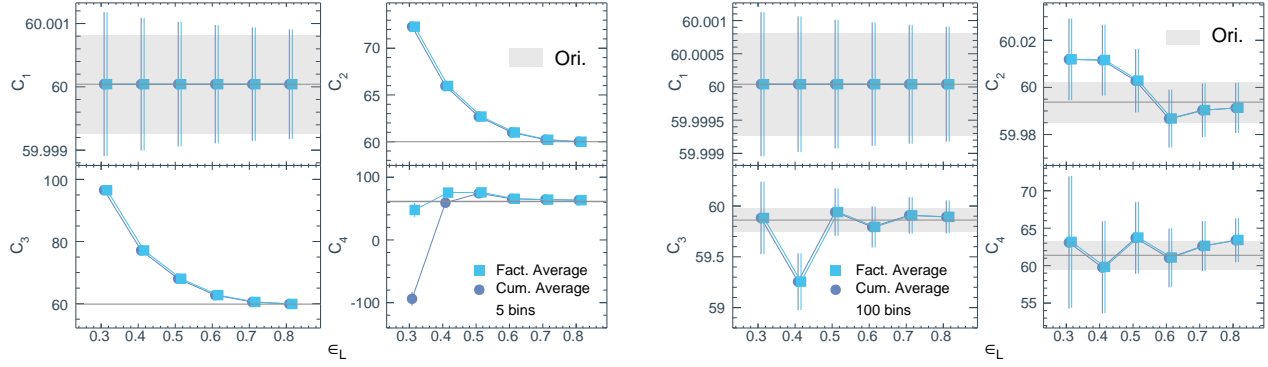


FIG. 3. Difference of the factorial moments average and the cumulants average. Simulation with 5 bins (left) and 100 bins (right). The efficiencies of events are selected randomly in the range  $(\epsilon_L, 0.8)$ . With finer efficiency bin (right), the difference of two method become smaller.

ter  $\lambda$ ) with the change of  $\Delta\epsilon$ . But the results start to show huge deviation for  $C_2$ ,  $C_3$  and  $C_4$ . Obviously, the correction failed even if the  $\Delta\epsilon$  is as less as 0.1 (When the event-by-event distribution shows no double peaks in Fig. 1).

Since we know that the event ensemble mixes up two types of distinctive event, which makes the correction failed for higher order cumulants. So, it is necessary to check whether the results can be improved when we do correction on each types respectively. In the following, we calculate cumulants on two types of event independently and correction them with their own measured efficiencies.

$$\epsilon_1 = \frac{\langle N \rangle_{\text{measure}}^{(1)}}{\langle N \rangle_{\text{input}}^{(1)}}, \quad \epsilon_2 = \frac{\langle N \rangle_{\text{measure}}^{(2)}}{\langle N \rangle_{\text{input}}^{(2)}}$$

The problem is how can we combine the corrected result of different types of events. The simulation of two types of events is the simplest case. Let's consider the measured distribution from combination of  $K$  types of events. We can find in the Section II A Equation (8) shows that the factorial moments  $f_r$  of superposed distribution is the weighted average of factorial moments  $f_r^{(i)}$  of each types. Therefore, the efficiency corrected factorial moments of superposed distribution is

$$F_r = \sum_{i=1}^k a_i \frac{f_r^{(i)}}{e^{k_{(i)}}} \quad (24)$$

The results are shown in Fig. 2 (right). As our expectation, the efficiency corrected cumulants follow the input values perfectly in all three cases.

As we have discussed in the Section II B, the cumulants of the superposition of different distributions (i.e. distribution corrected by mean efficiencies instead of true efficiencies) should be calculated from averaged factorial moments. The average on cumulants directly will introduce additional deviation. We show the difference of the factorial moments average and the cumulants average in Fig. 3. In Fig. 3, we perform a numerical simulation with 100M events. Instead of using 2 different efficiencies in the previous simulation,

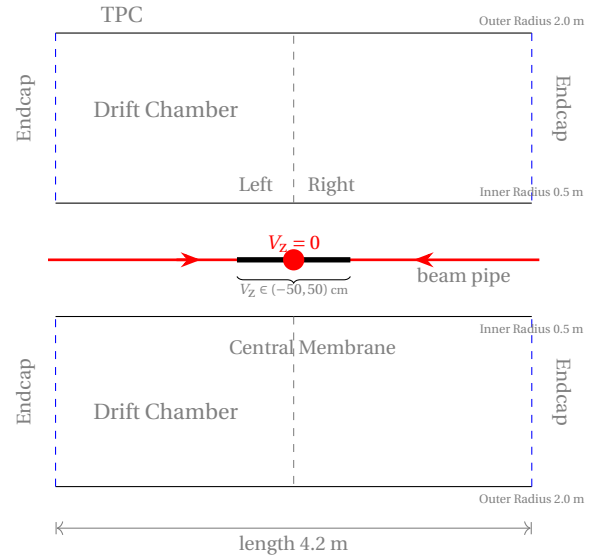


FIG. 4. A 2D sketch of the STAR TPC.

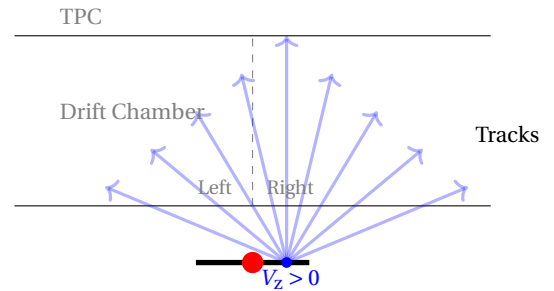


FIG. 5. Geometry sketch in UrQMD simulation. Each event from UrQMD has been assigned a random  $V_z$ .

each event has been randomly assigned an efficiency number, which is uniformly distributed in the range  $(\epsilon_L, 0.8)$ . To perform efficiency correction, the entire event sample has been divided into sub-event samples with the equal effi-

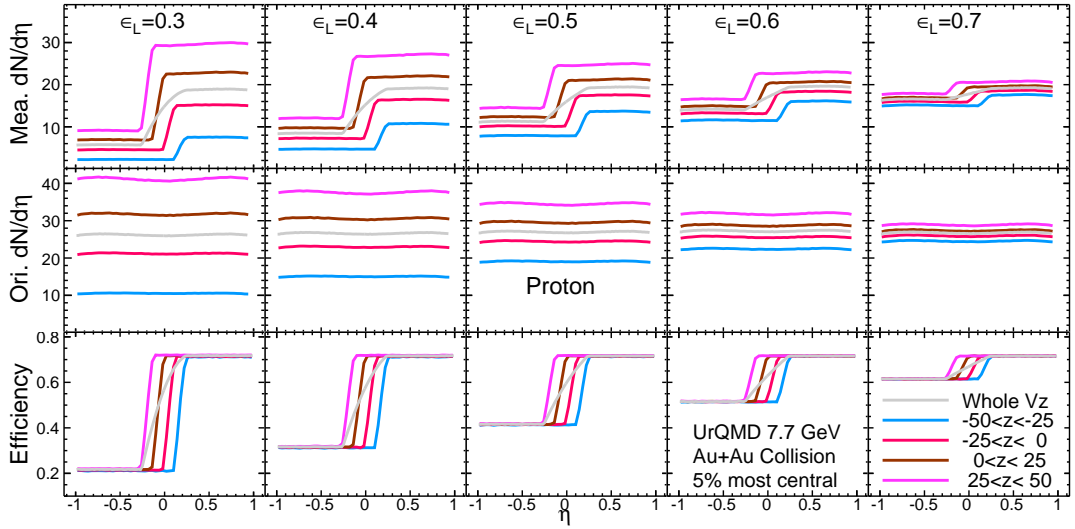


FIG. 6.  $dN/d\eta$  distribution (row 1: measured, row 2: original input) and the measurement efficiency (row 3). From left to right columns, the detecting efficiency of tracks in the left part of the drift chamber arising from 0.3 to 0.7, while the efficiency of tracks in the right part of the chamber fixed at 0.8. The  $\eta$  dependence of detecting efficiency can be represented by the ratio of the first and the second row.

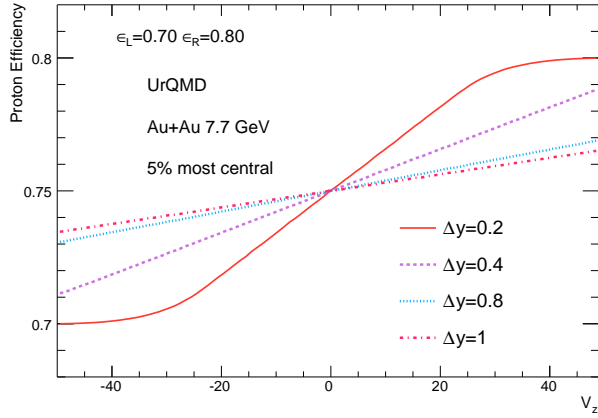


FIG. 7.  $V_z$  dependence of detecting efficiency within various rapidity coverage  $\Delta y$ . The wider  $\Delta y$  coverage corresponding to smoother slope in the figure.

ciency interval between  $(\epsilon_L, 0.8)$ . Efficiency correction for each sub-event sample has been done with the methods of factorial moments average and the cumulants average, respectively. We can infer from the left panel of Fig. 3 that with 5 efficiency bins (larger efficiency variations in each bin), the efficiency corrected results fail to reproduce the higher order input cumulants for both methods. However, for fourth order cumulant ( $C_4$ ), the average of factorial moments is closer to the original and the results from cumulants average method show large deviations. In order to reproduce the original cumulants, we have to reduce the efficiency variation and use more efficiency bins (with 100 bins in the right panel of Fig. 3). In finer efficiency bin, the factorial moment generating function  $G_F^{(i)}$  with mean efficiency becomes closer to its true value  $G_F$ , and also the additional

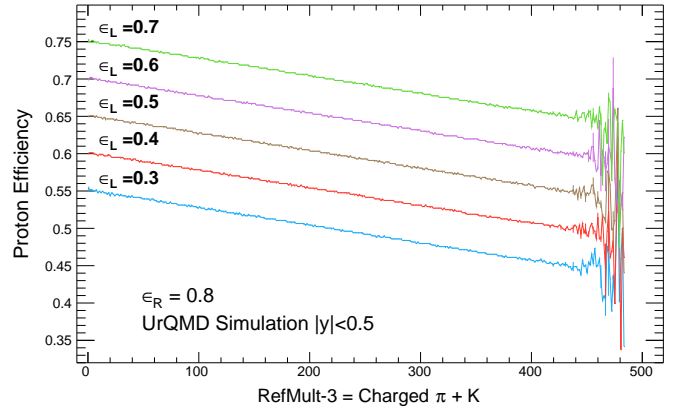


FIG. 8. Multiplicity dependence of detecting efficiency. The reference multiplicity in  $x$ -axis represents the multiplicity of charged  $\pi$  and  $K$  meson within  $|\eta| < 1$ . The different lines  $\epsilon_L$  in the figure represent various  $\epsilon_0$  in equation (25).

uncertainties of cumulants average become much smaller.

As a conclusion to this section, we demonstrate the effects of using mean efficiency in the efficiency correction for cumulants of multiplicity distributions. If the efficiency variation within the event sample is large, there is problem of using mean efficiency to do the efficiency corrections. To make precise and reliable efficiency correction, one has to be very careful of binning the events into various sub-event samples, in which the efficiency variation is relative small.

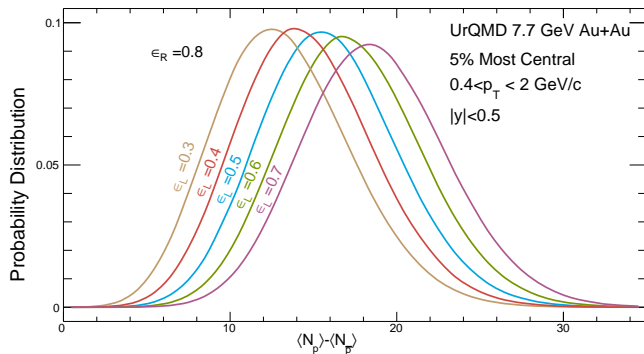


FIG. 9. Event-by-event distribution of net-proton. From left to right, the detecting efficiency of tracks in the left part of the drift chamber arising from 0.3 to 0.7, while the efficiency of tracks in the right part of the chamber fixed at 0.8.

#### IV. URQMD MODEL SIMULATION WITH STAR DETECTOR ACCEPTANCE

In this part, we want to check whether the failed correction in the last section can appear in real experiments or not. In STAR experiment, the particle identification and track reconstruction are usually done with a Time Projection Chamber [58] (TPC). The major structure of TPC is a cylinder drift chamber with a high voltage electrode in the center. The two endcaps of drift chamber are covered by the thin-gap, multiwire proportional chambers (MWPC). The passing particles in TPC will have energy loss due to the ionization of drifting electrons. By measuring the drift time and the number of electrons collected at endcaps, we can build the track of arrival particles and calculate their energy loss  $dE/dx$ . As shown in Fig. 4, the voltage electrode in the center (Central Membrane) divides the drift chamber into two subparts. Usually, the working condition of west and east side of TPC endcap are not essentially the same, which can result in different detecting efficiencies for the west and east TPC.

The  $z$ -coordination of primary vertex is described by an important event parameter  $V_z$ .  $V_z = 0$  indicates that the primary vertex locates at the longitudinal center of the TPC. In the simulation, the positive  $V_z$  indicates the primary vertex locates at the right. We also set a flat distribution of  $V_z$  within the range (-50 cm, 50 cm), which is similar case at RHIC BES low energies. In our discussion,  $V_z$  distributions are important because the efficiencies are unequal in the left and the right of the chamber. Since the particles from events with  $V_z < 0$  more likely travel into the left chamber, the mean efficiency of events with  $V_z < 0$  become different from that of events with  $V_z > 0$ . Obviously, we meet the situation that has been discussed in the Section III. In fact, the detecting efficiencies have been observed to change with  $V_z$  in real experiments.

#### A. Efficiency generation in UrQMD model

To investigate the effect from fluctuation of  $V_z$ . We have done a fast simulation with UrQMD model. UrQMD is a transport model which can simulate the nucleus-nucleus collision events [59]. The main idea is to give each UrQMD event a random  $V_z$  in the range  $-50 < V_z < 50$  cm. And then we can assign efficiency to each particle base on the  $V_z$  of the event and the  $\eta$  of the particle.

We simplify the geometry of TPC into a plane to emphasize the effects we are interest. Since we can judge which part of the drift chamber the particle will travel into by its pseudo-rapidity  $\eta$ , the tracks' azimuthal angle ( $\phi$ ) can be omitted from our study. Therefore, the scene we study can be sketched in Fig. 5. As shown in Fig. 5, the  $V_z$  of an event is randomly assigned. The angle ( $\theta$ ) between a track and the beam pipe line can be derived from pseudo-rapidity  $\eta$ .

Due to the magnetic field in TPC, particles in fact have helix trajectory when passing the chamber, however we can simplify this motion into straight line because we only care about in which part of the chamber the track will show up. Sometimes, there are tracks go through the central membrane. For the sake of clarity and simple, we suppose the entire track is in the left/right parts of the chamber if the end of this track is in the left/right parts of the chamber. Finally, we can assign detecting efficiencies  $\epsilon_L$  to tracks in the left chamber and  $\epsilon_R$  to tracks in the right chamber.

In addition to the effect of  $V_z$  fluctuation, the detecting efficiency is affected by the total multiplicity of charged particle. The multiplicity of charged particles are usually used as the reference to determine the centrality. It means the detecting efficiency must be different from central to peripheral collisions. Thus, we introduce a multiplicity dependence efficiency. The relation of total multiplicity and efficiency can be expressed as

$$\epsilon = \epsilon_0 - K_R N_{\text{mul}} \quad (25)$$

Where the  $\epsilon_0$  and the  $K_R$  is constant, and the  $N_{\text{mul}}$  is the total multiplicity of charged particles within  $|\eta| < 1$ . The minus sign before  $K_R$  indicates the detecting efficiency decreases with increasing total multiplicity. This effect can be introduced in the simulation by simply reducing the  $\epsilon_L$  and  $\epsilon_R$  by minus a factor  $K_R N_{\text{mul}}$ . For simplicity and clarity, we set the detecting efficiencies are flat as a function of  $p_T$  and the efficiencies of the  $p(\bar{p})$  are the same. Since we are interested in the efficiency fluctuations effects on net-proton cumulants, we didn't apply efficiencies to pions and kaons.

#### B. Results

In this work, we calculate the efficiency corrected cumulants of net-proton distributions in Au + Au collisions at  $\sqrt{s_{NN}} = 7.7$  GeV from UrQMD and select 0-5% most central events from the dataset, which is 2.0 million events. Collisions centrality is determined by charged particles within  $|\eta| < 1$  by excluding the proton and anti-protons. In Fig. 6,

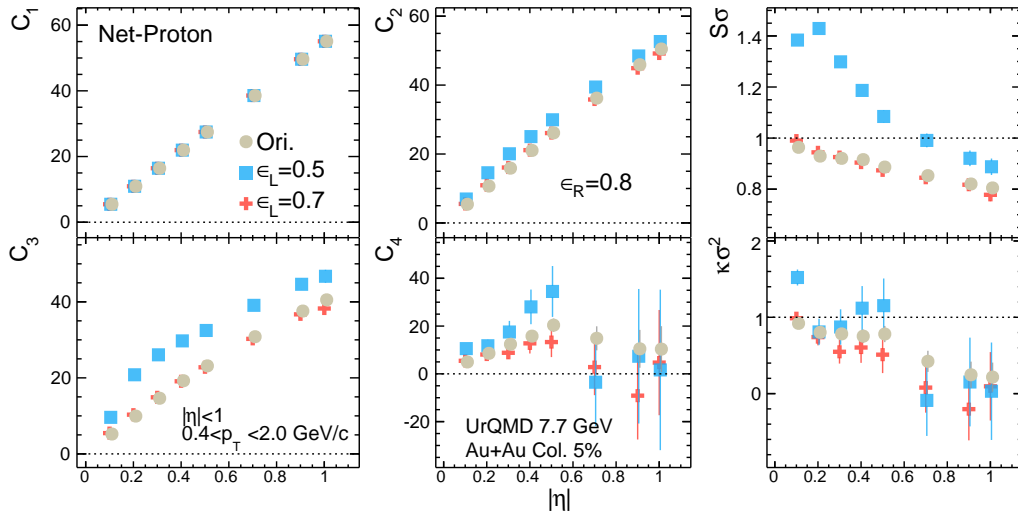


FIG. 10. Pseudo-rapidity dependence of efficiency corrected cumulants  $C_1$  to  $C_4$  (and their ratios  $S\sigma = C_3/C_2$ ,  $\kappa\sigma^2 = C_4/C_2$ ) of net-proton distributions. The mean efficiencies  $\langle\epsilon_p\rangle$ ,  $\langle\epsilon_{\bar{p}}\rangle$  are used in the efficiency corrections.

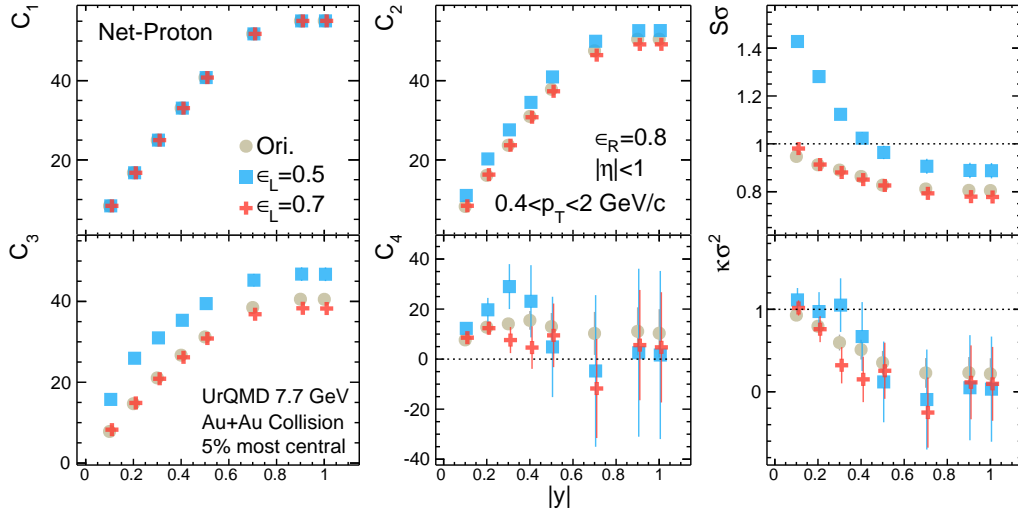


FIG. 11. Rapidity dependence of efficiency corrected cumulants  $C_1$  to  $C_4$  (and their ratios  $S\sigma = C_3/C_2$ ,  $\kappa\sigma^2 = C_4/C_2$ ) of net-proton distributions. The mean efficiencies  $\langle\epsilon_p\rangle$ ,  $\langle\epsilon_{\bar{p}}\rangle$  are used in the efficiency corrections.

we show the proton  $dN/d\eta$  distribution for measured data (with  $V_z$  fluctuation and detecting efficiencies) and original UrQMD data within pseudo-rapidity coverage  $|\eta| < 1.0$ , which is the same coverage of TPC of STAR detector. Different colors of lines in Fig. 6 represent the  $dN/d\eta$  distributions of protons within various  $V_z$  ranges. In the columns from left to right, we gradually increase the efficiency of tracks in left part of the chamber (corresponding to  $\eta < 0$  from  $\epsilon_L = 0.3$  to  $\epsilon_L = 0.7$ , while we fix the efficiency in right part of the chamber at  $\epsilon_R = 0.8$ ). Thus, we can evaluate the efficiency fluctuation effects when we enlarge or reduce the difference of  $\epsilon_L$  and  $\epsilon_R$ .

We can learn from Fig. 6 that the proton  $dN/d\eta$  distributions are asymmetry in positive and negative  $\eta$  region, while the distributions of original input are flat. The detecting ef-

ficiencies of particles can be expressed as the ratio of the first and the second row. We found that when we narrow the  $V_z$  bin width, the slope from negative  $\eta$  to positive  $\eta$  become steeper. On the contrary, wider  $V_z$  bin shows smaller slope. It implies that wider  $V_z$  bins mix up more distinctive events.

The relations between rapidity coverage,  $V_z$  and the proton efficiency are shown in Fig. 7. In this figure, the mean proton efficiency within various rapidity coverage  $\Delta y$  is plotted as a function of  $V_z$ . The efficiencies for  $V_z > 0$  are larger than those of  $V_z < 0$ , which is consistent with our setting. When the  $\Delta y$  is smaller, particles are more likely to concentrate in left or right chamber. Therefore, the slope from  $V_z < 0$  to  $V_z > 0$  is steeper. When  $\Delta y$  is larger, particles are more dispersed into different chamber parts, what leads

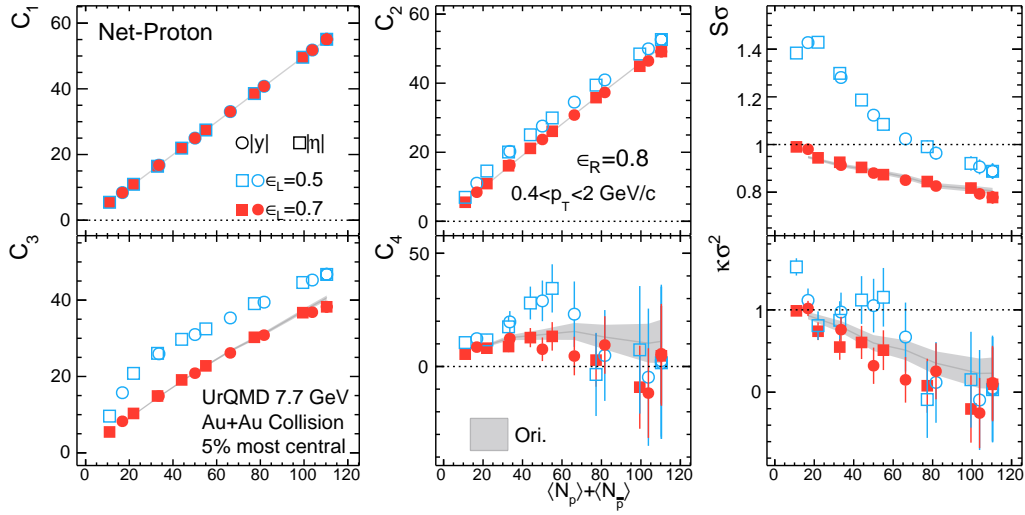


FIG. 12. Net-proton cumulants and cumulant ratios as functions of mean total-proton number  $\langle N_p \rangle + \langle N_{\bar{p}} \rangle$ .

to a smooth transition from  $V_z < 0$  to  $V_z > 0$ .

The effect on detecting efficiency from total multiplicity is shown in Fig. 8, where the proton mean efficiency is plotted as a function of the multiplicity of charged  $\pi$  and  $K$ . Experimentally, instead of using wider centrality bins to calculate the cumulants, the net-proton cumulants are calculated in individual reference multiplicity bins to reduce the volume fluctuation which arising from the uncertainty of collision geometry. This is a technique so called centrality bin width correction (CBWC) [60]. The reference multiplicity equals to the multiplicity of charged  $\pi$  and  $K$  within  $|\eta| < 1$ . From the previous discussion, the mean efficiency should be different across centralities and reference multiplicity bins.

In Fig. 6–8, we obtained the proton mean efficiency in simulation and thus we can carry out the efficiency correction to the net-proton cumulants. We first check the event-by-event distributions of measured net-proton number in simulation. In Fig. 9, we found that the shapes of the distributions show no significant changes when we enlarge the difference between  $\epsilon_L$  and  $\epsilon_R$ . The similar shape of distributions is due to the continuous distributions of  $V_z$ . And the event-by-event distribution of mean net-proton number is the superposition of events within the whole  $V_z$  range.

We show the efficiency corrected net-proton cumulants  $C_1$  to  $C_4$  (and their ratios  $S\sigma = C_3/C_2$ ,  $\kappa\sigma^2 = C_4/C_2$ ) within various pseudo-rapidity and rapidity coverages in Fig. 10–11. The mean efficiencies of proton and anti-protons are used in the efficiency corrections. As we suppose in our previous work that the cumulants in various rapidity or pseudo-rapidity acceptance have  $\langle N_p \rangle$  scaling behavior (or  $\langle N_p \rangle + \langle N_{\bar{p}} \rangle$  scaling) [61], we also plot the cumulants and their ratios as functions of mean total-proton number  $\langle N_p \rangle + \langle N_{\bar{p}} \rangle$  in Fig. 12, where the cumulants within various  $\Delta\eta$  or  $\Delta y$  acceptance show unified trend to the mean net-proton number (or total-proton number). The original results which computed from original input without detect-

ing efficiency are shown as solid gray line in the figure. The measured cumulants are represented by colored markers. We found that the efficiency corrected cumulants coincide to the original results when the efficiencies of left and right part of chamber are close to each other. However, when the difference between  $\epsilon_L$  and  $\epsilon_R$  become larger (i.e. the case  $\epsilon_L = 0.5$ ,  $\epsilon_R = 0.8$ ), the efficiency correction failed for the higher order cumulants as we found in the Section III, and the deviations grow rapidly with the difference.

The simulation confirms that using mean efficiency in correction can produce inaccurate results and the effect of efficiencies fluctuation is not negligible. Fortunately, the deviation is not negligible only when the efficiency difference  $\Delta\epsilon$  become unrealistic large compare to real experiments. In the cases when the  $\Delta\epsilon$  is less than 0.2, the efficiency corrected cumulants coincide to input results within statistical uncertainties.

### C. $V_z$ bin correction

The results shown in Fig. 6 suggest that wider  $V_z$  bins mix up more distinctive events, thus we can perform the efficiency correction within smaller  $V_z$  bins.

The method to perform the correction of  $V_z$  fluctuation is analogous to what we have done in the Section III. We may suppose that event with different  $V_z$  has its own mean efficiency. Therefore, the measured distribution is the superposed distribution from all  $V_z$  ranges, and the superposed distribution from events with different efficiencies. Mean efficiencies of smaller  $V_z$  bins can be obtained from Monte Carlo embedding procedure. Suppose the efficiency corrected factorial moments at  $V_z$  is  $F_r(V_z)$ , we can write the average result as equation (24)

$$\tilde{F}_r = \int_{V_z} F_r(V_z) dV_z$$

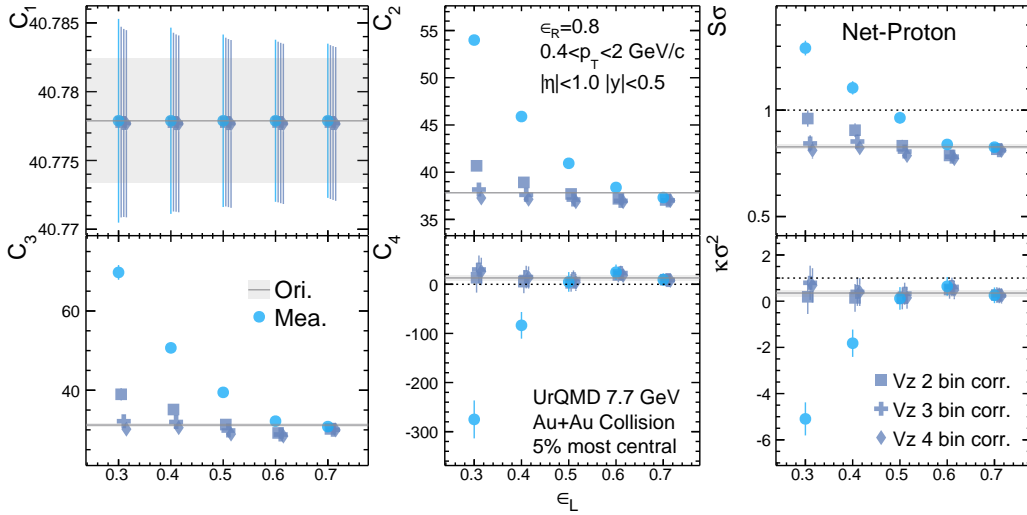


FIG. 13. The efficiency corrected net-proton cumulants with/without  $V_z$  bin average in various  $\Delta\epsilon$ . The  $x$ -axis is the efficiency  $\epsilon_L$  in the left chamber, and the  $\epsilon_R$  is fixed at 0.8. The result without  $V_z$  bin average (full circle marker) show large deviations from original results.

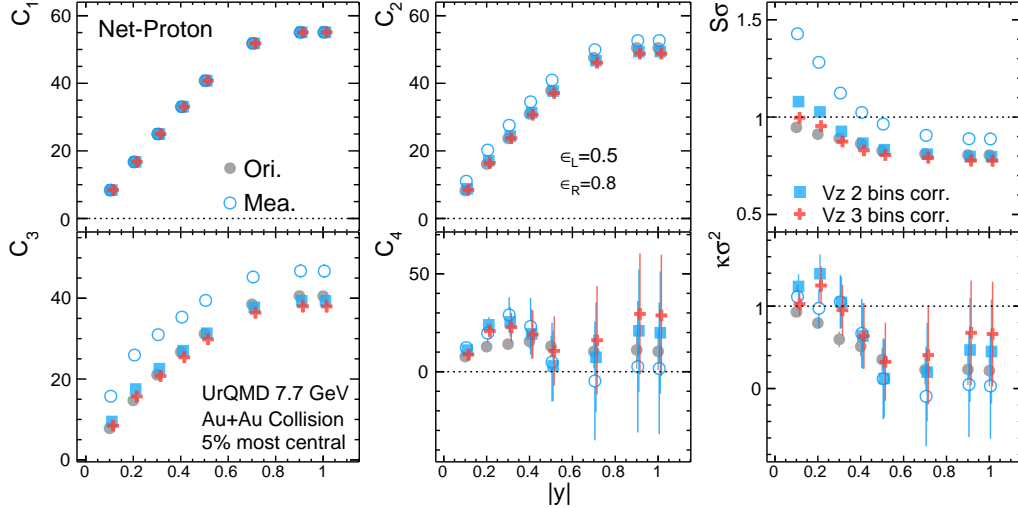


FIG. 14. Rapidity dependence of efficiency corrected net-proton cumulants with/without  $V_z$  bin average. The precision of correction has been significantly improved by average of 2  $V_z$  bins. When the  $\Delta\epsilon = \epsilon_R - \epsilon_L$  is larger, finer  $V_z$  bins (3 bins) are required.

The statistical error is evaluated by propagation of standard error.

We first investigate the effect of  $V_z$  bin correction with different  $\Delta\epsilon$  and different  $V_z$  bin width. Fig. 13 shows that when  $\Delta\epsilon = \epsilon_R - \epsilon_L$  is large, results corrected by mean efficiency show large deviations from the input results. For the  $V_z$  bin correction, we setup 2 or 3, 4  $V_z$  bins with equal interval in the range of  $(-50 \text{ cm}, 50 \text{ cm})$  to do the efficiency correction. We found that the  $V_z$  bin correction can significantly improve the results of high order cumulants, especially in the case where  $\Delta\epsilon$  is large. Finer  $V_z$  bin is important when  $\Delta\epsilon$  is large. We also learn from Fig. 13 that efficiency corrected by 2  $V_z$  bins has already shows great improvement. But the effect of  $V_z$  bin correction may depend on the rapidity acceptance, since we found in Fig. 7 that smaller rapidity acceptance  $\Delta y$  show a steeper slope on the  $V_z$  dependence of

efficiency. In Fig. 14 we show 2 and 3  $V_z$  bins corrected result within various  $y$  cuts. When  $|y|$  cut is small, result corrected by 3 bins is better than 2 bins. But the discrepancy is not significant for larger  $|y|$  cut. The reason can be explained by the fact that when  $|y|$  cut is large, particles are dispersed more evenly in two drifting chambers, so the efficiency depends less on  $V_z$ .

## V. SUMMARY

In heavy ion collision, the cumulants of event-by-event multiplicity of conserved charge have been used as sensitive observables to probe the QCD phase transition and the critical point. Since experiments have finite acceptance and detector efficiency, the measured distribution should be cor-

rected for detecting efficiency in analysis.

Particle efficiencies of events measured with different experimental conditions should be different. We called this effect as event-by-event efficiency fluctuations. The final event-by-event multiplicity distributions should be the superposed distributions of various type of events measured under different conditions. However, the efficiency correction is done with a mean efficiency of the event sample. Mean efficiencies obtained from Monte Carlo embedding procedure have been used to do the efficiency correction for cumulants. The mean efficiencies reflect the net contribution from the acceptance, tracking efficiency and other effects. We have shown the relation between the factorial moments of the superposed distribution and the factorial moments from individual distributions (i.e. the distribution with different efficiencies). We find that the superposed factorial moments is the weighted average of the individual factorial moments, and the mean efficiency cannot restore the original input, since the efficiency is fluctuating across the various distributions. So we suggest that one should be very careful of binning the events into various sub-event samples, in which the efficiency variation is relative small.

A numerical simulation which combines two types of events with different efficiencies has shown that the correction done with mean efficiency can have significant deviation from the original input. And a more concrete simulation with UrQMD model indicates that the similar effects can exist in real experiments. In the UrQMD simulation, we consider the event-by-event fluctuation of  $z$ -coordination of collision vertex ( $V_z$ ). We also introduce the different working condition of detectors at the west and east endcap of the detector (TPC), which can lead to unequal detecting efficiencies of the tracks in the west and east subpart of the chamber. We show that the event-by-event efficiency fluctuation effects can cause the efficiency corrected cumulants using mean efficiencies deviating from original input. However, when the efficiency fluctuation is at the level of real experiments which is much smaller than our settings, the deviation can be negligible. We also have tried to reduce the efficiency variation by introducing  $V_z$  bin average method, which can significantly improve the precision of the efficiency correction.

The event-by-event efficiency fluctuation implemented in this simulation, is not the only sources that can exist in the real experiments. For example, other sources, such as that the variation of the detector performance as a function of time and bad events outliers in the multiplicity distributions. To obtain precise and reliable efficiency corrected cumulants, one needs to have a careful studies on the event selection and classification to make sure the event-by-event efficiency fluctuations is small. Our studies provide an effective method to improve the precision of efficiency correction for cumulant analysis in relativistic heavy-ion collision experiments.

## ACKNOWLEDGMENTS

The work was supported in part by the MoST of China 973-Project No.2015CB856901, NSFC under grant No. 11575069.

## VI. APPENDIX

### A. Efficiency correction for factorial moments

The factorial moments generating function is

$$G_F(s) = \sum_{n=0}^{\infty} P(n) s^n \quad (26)$$

Where the  $n$  is the value of the stochastic variable. And the  $P(n)$  is the probability density function. The summation can also be expressed as

$$G_F(s) = \langle s^n \rangle$$

Therefore the  $r$ -th factorial moment of  $n$  is

$$\begin{aligned} F_r &= \left. \frac{\partial^r}{\partial s^r} G_F(s) \right|_{s=1} \\ &= \sum_{n=r}^{\infty} P(n) n(n-1)(n-2)\cdots(n-r+1) \\ &= \langle n(n-1)\cdots(n-r+1) \rangle \end{aligned} \quad (27)$$

The probability of detecting  $n$  particles ( $p(n)$ ) is given by binominal distribution  $B_N(n, \epsilon)$ , where  $N$  is the number of input particle and the  $\epsilon$  is the efficiency.

$$\begin{aligned} p(n) &= \sum_{N=n}^{\infty} P(N) B_N(n, \epsilon) \\ &= \sum_{N=n}^{\infty} P(N) \binom{N}{n} \epsilon^n (1-\epsilon)^{N-n} \end{aligned} \quad (28)$$

The generating function of measured factorial moments is then

$$\begin{aligned} G_f(s) &= \sum_{n=0}^{\infty} p(n) s^n \\ &= \sum_{n=0}^{\infty} \sum_{N=n}^{\infty} P(N) \binom{N}{n} \epsilon^n (1-\epsilon)^{N-n} s^n \\ &= \sum_{N=0}^{\infty} P(N) \sum_{n=0}^N \binom{N}{n} \epsilon^n (1-\epsilon)^{N-n} s^n \\ &= \sum_{N=0}^{\infty} P(N) \sum_{n=0}^N \binom{N}{n} (\epsilon s)^n (1-\epsilon)^{N-n} \end{aligned} \quad (29)$$

The last line can be simplified by binomial theorem

$$\sum_{n=0}^N \binom{N}{n} (\epsilon s)^n (1-\epsilon)^{N-n} = [\epsilon s + (1-\epsilon)]^N$$

We then have

$$\begin{aligned} G_f(s) &= \sum_{N=0}^{\infty} P(N) [1 + \epsilon(s-1)]^N \\ &= \sum_{N=0}^{\infty} P(N) s'^N = G_F(s') \end{aligned} \quad (30)$$

Where  $s' = [1 + \epsilon(s-1)]$ . We then have the relation between measured factorial moments  $f_r$  and original factorial moments  $F_r$

$$\begin{aligned} f_r &= \left. \frac{\partial^r}{\partial s^r} G_f(s) \right|_{s=1} \\ &= \left. \frac{\partial^r}{\partial s^r} \sum_{N=0}^{\infty} P(N) [1 + \epsilon(s-1)]^N \right|_{s=1} \\ &= \sum_{N=r}^{\infty} \epsilon^r P(N) N(N-1) \cdots (N-r+1) = \epsilon^r F_r \end{aligned} \quad (31)$$

## B. Multivariate factorial moments

In the paper, we use multivariate factorial moments to describe the net-proton number. The net-proton factorial moments has 2 dimensions which describes proton and anti-proton number respectively. The generating function of  $q$ -dimensional factorial moments is an extension to equation (26)

$$G_F(\mathbf{t}) = \prod_q \sum_{n_q=0}^{\infty} P_q(n_q) t_q^{n_q} \quad (32)$$

Therefore

$$\begin{aligned} F_r &= \prod_q \left. \frac{\partial^{r_q}}{\partial t_q^{r_q}} \sum_{n_q=0}^{\infty} P_q(n_q) t_q^{n_q} \right|_{t_q=1} \\ &= \left\langle \prod_q (t_q)_{r_q} \right\rangle \end{aligned} \quad (33)$$

Where the symbol  $(t_q)_{r_q}$  is falling factorial

$$(t_q)_{r_q} = t_q(t_q-1)(t_q-2) \cdots (t_q-r_q+1)$$

The detecting probability density function for each kind of particles is identical to equation (28)

$$p_q(n_q) = \sum_{N_q=n_q}^{\infty} P_q(N_q) B_{N_q}(n_q, \epsilon_q) \quad (34)$$

Therefore the generating function for measured factorial moments is given by equation (29)

$$\begin{aligned} G_f(\mathbf{t}) &= \prod_q \sum_{n_q=0}^{\infty} p_q(n_q) t_q^{n_q} \\ &= \prod_q \sum_{n_q=0}^{\infty} \sum_{N_q=n_q}^{\infty} P_q(N_q) B_{N_q}(n_q, \epsilon_q) \\ &= \prod_q P_q(N_q) [1 + \epsilon_q(t_q-1)]^{N_q-n_q} \end{aligned} \quad (35)$$

Thus, the efficiency correction relation is similar to equation (31)

$$f_r = \left( \prod_q \epsilon_q^{r_q} \right) F_r \quad (36)$$

The conversion from  $q$ -dimensional factorial moments to  $q$ -dimensional moments is similar to equation (3)

$$\left\langle \prod_q N_q^{r_q} \right\rangle = \sum_{i_1=0}^{r_1} \cdots \sum_{i_q=0}^{r_q} s_2(r_1, i_1) \cdots s_2(r_q, i_q) F_{r_1, r_2, \dots, r_q} \quad (37)$$

With  $q$ -dimensional moments we can write down moments of any combination of  $q$  kinds of particles, for example, the moments of net-proton number is

$$\begin{aligned} \langle (N_1 - N_2)^r \rangle &= \left\langle \sum_{i=0}^r \binom{r}{i} (-1)^i N_1^{r-i} N_2^i \right\rangle \\ &= \sum_{i=0}^r \binom{r}{i} (-1)^i \langle N_1^{r-i} N_2^i \rangle \\ &= \sum_{i=0}^r \binom{r}{i} (-1)^i \sum_{k_1=0}^{r-i} \sum_{k_2=0}^i s_2(r-i, k_1) s_2(i, k_2) F_{k_1, k_2} \end{aligned} \quad (38)$$

And the cumulants of net-proton number is given by equation (1) directly.

- 
- [1] Y. Aoki, G. Endrodi, Z. Fodor, S. D. Katz, and K. K. Szabo, *Nature* **443**, 675 (2006), arXiv:hep-lat/0611014 [hep-lat].  
 [2] B. J. Schaefer and M. Wagner, *Phys. Rev.* **D85**, 034027 (2012), arXiv:1111.6871 [hep-ph].  
 [3] M. Asakawa, S. Ejiri, and M. Kitazawa, *Phys. Rev. Lett.* **103**, 262301 (2009), arXiv:0904.2089 [nucl-th].

- [4] G. Endrodi, Z. Fodor, S. D. Katz, and K. K. Szabo, *JHEP* **04**, 001 (2011), arXiv:1102.1356 [hep-lat].  
 [5] M. A. Stephanov, *Non-perturbative quantum chromodynamics. Proceedings, 8th Workshop, Paris, France, June 7-11, 2004*, *Prog. Theor. Phys. Suppl.* **153**, 139 (2004), [*Int. J. Mod. Phys.A*20,4387(2005)], arXiv:hep-ph/0402115 [hep-ph].

- [6] J.-W. Chen, J. Deng, H. Kohyama, and L. Labun, Phys. Rev. **D93**, 034037 (2016), arXiv:1509.04968 [hep-ph].
- [7] V. Vovchenko, D. V. Anchishkin, M. I. Gorenstein, and R. V. Poberezhnyuk, Phys. Rev. **C92**, 054901 (2015), arXiv:1506.05763 [nucl-th].
- [8] V. Vovchenko, M. I. Gorenstein, and H. Stoecker, Phys. Rev. Lett. **118**, 182301 (2017), arXiv:1609.03975 [hep-ph].
- [9] W. Fan, X. Luo, and H. Zong, (2017), arXiv:1702.08674 [hep-ph].
- [10] K. Fukushima, Phys. Rev. **C91**, 044910 (2015), arXiv:1409.0698 [hep-ph].
- [11] F. Karsch and K. Redlich, Phys. Lett. **B695**, 136 (2011), arXiv:1007.2581 [hep-ph].
- [12] P. Braun-Munzinger, B. Friman, F. Karsch, K. Redlich, and V. Skokov, Phys. Rev. **C84**, 064911 (2011), arXiv:1107.4267 [hep-ph].
- [13] R. V. Gavai and S. Gupta, Phys. Lett. **B696**, 459 (2011), arXiv:1001.3796 [hep-lat].
- [14] S. Borsanyi, Z. Fodor, S. D. Katz, S. Krieg, C. Ratti, and K. K. Szabo, Phys. Rev. Lett. **111**, 062005 (2013), arXiv:1305.5161 [hep-lat].
- [15] A. Bazavov *et al.*, Phys. Rev. Lett. **109**, 192302 (2012), arXiv:1208.1220 [hep-lat].
- [16] K. Morita, B. Friman, and K. Redlich, Phys. Lett. **B741**, 178 (2015), arXiv:1402.5982 [hep-ph].
- [17] L. Jiang, P. Li, and H. Song, *Proceedings, 25th International Conference on Ultra-Relativistic Nucleus-Nucleus Collisions (Quark Matter 2015): Kobe, Japan, September 27-October 3, 2015*, Nucl. Phys. **A956**, 360 (2016), arXiv:1512.07373 [nucl-th].
- [18] L. Jiang, P. Li, and H. Song, Phys. Rev. **C94**, 024918 (2016), arXiv:1512.06164 [nucl-th].
- [19] L. Adamczyk *et al.* (STAR), Phys. Rev. Lett. **113**, 092301 (2014), arXiv:1402.1558 [nucl-ex].
- [20] P. Alba, W. Alberico, R. Bellwied, M. Bluhm, V. Mantovani Sarti, M. Nahrgang, and C. Ratti, Phys. Lett. **B738**, 305 (2014), arXiv:1403.4903 [hep-ph].
- [21] X. Luo and N. Xu, Nucl. Sci. Tech. **28**, 112 (2017), arXiv:1701.02105 [nucl-ex].
- [22] S. Ejiri, F. Karsch, and K. Redlich, Phys. Lett. **B633**, 275 (2006), arXiv:hep-ph/0509051 [hep-ph].
- [23] M. A. Stephanov, K. Rajagopal, and E. V. Shuryak, Phys. Rev. **D60**, 114028 (1999), arXiv:hep-ph/9903292 [hep-ph].
- [24] M. A. Stephanov, Phys. Rev. Lett. **102**, 032301 (2009), arXiv:0809.3450 [hep-ph].
- [25] M. A. Stephanov, Phys. Rev. Lett. **107**, 052301 (2011), arXiv:1104.1627 [hep-ph].
- [26] A. Bzdak, V. Koch, and N. Strodthoff, Phys. Rev. **C95**, 054906 (2017), arXiv:1607.07375 [nucl-th].
- [27] X. Luo (STAR), *Proceedings, 23rd International Conference on Ultrarelativistic Nucleus-Nucleus Collisions: Quark Matter 2012 (QM 2012): Washington, DC, USA, August 13-18, 2012*, Nucl. Phys. **A904-905**, 911c (2013), [Central Eur. J. Phys.10,1372(2012)], arXiv:1210.5573 [nucl-ex].
- [28] B. Friman, *Proceedings, 45 Years of Nuclear Theory at Stony Brook: A Tribute to Gerald E. Brown: Stony Brook, NY, USA, November 24-26, 2013*, Nucl. Phys. **A928**, 198 (2014), arXiv:1404.7471 [nucl-th].
- [29] M. Kitazawa and M. Asakawa, Phys. Rev. **C85**, 021901 (2012), arXiv:1107.2755 [nucl-th].
- [30] M. Kitazawa and M. Asakawa, Phys. Rev. **C86**, 024904 (2012), [Erratum: Phys. Rev.C86,069902(2012)], arXiv:1205.3292 [nucl-th].
- [31] B. Friman, F. Karsch, K. Redlich, and V. Skokov, Eur. Phys. J. **C71**, 1694 (2011), arXiv:1103.3511 [hep-ph].
- [32] M. Cheng *et al.*, Phys. Rev. **D79**, 074505 (2009), arXiv:0811.1006 [hep-lat].
- [33] X. Luo, *Proceedings, 25th International Conference on Ultra-Relativistic Nucleus-Nucleus Collisions (Quark Matter 2015): Kobe, Japan, September 27-October 3, 2015*, Nucl. Phys. **A956**, 75 (2016), arXiv:1512.09215 [nucl-ex].
- [34] M. M. Aggarwal *et al.* (STAR), (2010), arXiv:1007.2613 [nucl-ex].
- [35] A. Zhao, X. Luo, and H. Zong, Eur. Phys. J. **C77**, 207 (2017), arXiv:1609.01416 [nucl-th].
- [36] S. Jeon and V. Koch, Phys. Rev. Lett. **83**, 5435 (1999), arXiv:nucl-th/9906074 [nucl-th].
- [37] M. Asakawa, U. W. Heinz, and B. Muller, Phys. Rev. Lett. **85**, 2072 (2000), arXiv:hep-ph/0003169 [hep-ph].
- [38] J. Xu, *Proceedings, 32th Winter Workshop on Nuclear Dynamics (WWND 2016): Guadeloupe, French West Indies, February 26-March 5, 2016*, J. Phys. Conf. Ser. **736**, 012002 (2016), arXiv:1611.07134 [hep-ex].
- [39] J. Xu, S. Yu, F. Liu, and X. Luo, Phys. Rev. **C94**, 024901 (2016), arXiv:1606.03900 [nucl-ex].
- [40] L. Adamczyk *et al.* (STAR), (2017), arXiv:1709.00773 [nucl-ex].
- [41] M. M. Aggarwal *et al.* (STAR), Phys. Rev. Lett. **105**, 022302 (2010), arXiv:1004.4959 [nucl-ex].
- [42] L. Adamczyk *et al.* (STAR), Phys. Rev. Lett. **112**, 032302 (2014), arXiv:1309.5681 [nucl-ex].
- [43] X. Luo (STAR), *Proceedings, 9th International Workshop on Critical Point and Onset of Deconfinement (CPOD 2014): Bielefeld, Germany, November 17-21, 2014*, PoS **CPOD2014**, 019 (2015), arXiv:1503.02558 [nucl-ex].
- [44] S. Mukherjee, R. Venugopalan, and Y. Yin, Phys. Rev. Lett. **117**, 222301 (2016), arXiv:1605.09341 [hep-ph].
- [45] S. Mukherjee, R. Venugopalan, and Y. Yin, Phys. Rev. **C92**, 034912 (2015), arXiv:1506.00645 [hep-ph].
- [46] M. Nahrgang, M. Bluhm, P. Alba, R. Bellwied, and C. Ratti, Eur. Phys. J. **C75**, 573 (2015), arXiv:1402.1238 [hep-ph].
- [47] A. Bzdak, V. Koch, and V. Skokov, Phys. Rev. **C87**, 014901 (2013), arXiv:1203.4529 [hep-ph].
- [48] B. Ling and M. A. Stephanov, Phys. Rev. **C93**, 034915 (2016), arXiv:1512.09125 [nucl-th].
- [49] B. Berdnikov and K. Rajagopal, Phys. Rev. **D61**, 105017 (2000), arXiv:hep-ph/9912274 [hep-ph].
- [50] S. He, X. Luo, Y. Nara, S. Esumi, and N. Xu, Phys. Lett. **B762**, 296 (2016), arXiv:1607.06376 [nucl-ex].
- [51] M. Nahrgang, T. Schuster, M. Mitrovski, R. Stock, and M. Bleicher, Eur. Phys. J. **C72**, 2143 (2012), arXiv:0903.2911 [hep-ph].
- [52] M. Sakaida, M. Asakawa, and M. Kitazawa, Phys. Rev. **C90**, 064911 (2014), arXiv:1409.6866 [nucl-th].
- [53] B. I. Abelev *et al.* (STAR), Phys. Rev. **C79**, 034909 (2009), arXiv:0808.2041 [nucl-ex].
- [54] A. Bzdak and V. Koch, Phys. Rev. **C86**, 044904 (2012), arXiv:1206.4286 [nucl-th].
- [55] X. Luo, Phys. Rev. **C91**, 034907 (2015), [Erratum: Phys. Rev.C94,no.5,059901(2016)], arXiv:1410.3914 [physics.data-an].
- [56] M. Kitazawa and X. Luo, Phys. Rev. **C96**, 024910 (2017), arXiv:1704.04909 [nucl-th].
- [57] X. Luo, J. Phys. **G39**, 025008 (2012), arXiv:1109.0593 [physics.data-an].
- [58] W. R. Leo, *Techniques for Nuclear and Particle Physics Experiments: A How to Approach* (1987).
- [59] S. A. Bass *et al.*, Prog. Part. Nucl. Phys. **41**, 255 (1998), [Prog. Part. Nucl. Phys.41,225(1998)], arXiv:nucl-th/9803035 [nucl-

th].

[60] X. Luo, J. Xu, B. Mohanty, and N. Xu, *J. Phys.* **G40**, 105104 (2013), arXiv:1302.2332 [nucl-ex].  
[61] S. He and X. Luo, *Phys. Lett.* **B774**, 623 (2017), arXiv:1704.00423 [nucl-ex].